

Short communication

## High-temperature characteristics of advanced Ni-MH batteries using nickel electrodes containing $\text{CaF}_2$

Xuezeng Zhang<sup>a</sup>, Zhixin Gong<sup>a</sup>, Shumei Zhao<sup>a</sup>, Mingming Geng<sup>b</sup>,  
Yan Wang<sup>c</sup>, Derek O. Northwood<sup>c,\*</sup>

<sup>a</sup> Peace Bay Power Sources Co. Ltd., Tianjin 300384, PR China

<sup>b</sup> PowerGenix, San Diego, CA 92131-1109, USA

<sup>c</sup> MAME Department, University of Windsor, Windsor, Ont. N9B 3P4, Canada

Received 16 July 2007; received in revised form 17 August 2007; accepted 30 August 2007

Available online 7 September 2007

### Abstract

The high-temperature charge acceptance of Ni-MH batteries has been improved through the addition of calcium fluoride to the pasted nickel hydroxide electrode made using spherical  $\text{Co}(\text{OH})_2$ -coated nickel hydroxide powder. The charge acceptance of the Ni-MH battery at 60 °C is over 95% at 1 C charge/discharge rates. The charge acceptance at 60 °C remains at over 90% through 10 cycles. The use of  $\text{Co}(\text{OH})_2$ -coated  $\text{Ni}(\text{OH})_2$  plus a  $\text{CaF}_2$  addition to the positive electrode also significantly improved the high-temperature stability in terms of reduced gas evolution.

© 2007 Elsevier B.V. All rights reserved.

**Keywords:** Nickel-metal hydride battery; High-temperature charge acceptance;  $\text{Co}(\text{OH})_2$ -coated nickel hydroxide; Cycle lifetime

### 1. Introduction

Advanced nickel-metal hydride (Ni-MH) batteries have found application in power tools, UPS, electric vehicles (EV) and hybrid electric vehicles (HEVs) in the past several years. The technical strengths of Ni-MH battery systems are recognized as high-power capability, long-term durability and high charge/discharge efficiency. Despite the emergence of lithium ion batteries and small, portable fuel cells, Ni-MH batteries continue to receive much attention because almost all of the commercial HEVs employ Ni-MH batteries due to their better combination of power output, capacity, life, reliability and cost [1–8].

Co or Co compounds have been widely adopted as an addition to the nickel hydroxide electrode because Co can transform to  $\text{CoOOH}$  during the first activation charging, which supplies a conductive network for the positive electrode. Also, the addition of cobalt in  $\text{Ni}(\text{OH})_2$  lattice has been shown to increase the oxygen evolution potential, thereby improving the  $\text{Ni}(\text{OH})_2$  active material utilization and cycle life [9–15]. Other additions,

including Ba, Mn, Cu, Zn and Cd, have also been studied in order to increase the performance of Ni-MH batteries [13–17].

To meet the requirement for HEV and power tool applications, Ni-MH batteries should be able to operate at high temperatures (>50 °C) without significant deterioration in performance. However, the charge efficiency of the positive electrodes significantly declines because of oxygen evolution at high temperatures, leading to the overall poor performance of Ni-MH batteries. Much work has been done on additions to improve the high temperature charge–discharge characteristics of the positive electrode because the performance of Ni-MH batteries is strongly influenced by the positive Ni electrode which determines the cell capacity [10]. Additions of cobalt oxide [9,18–20], zinc oxide [21], and lanthanide oxides [22,23] have been made to the positive electrodes in order to increase the high-temperature performance of Ni-MH batteries. Also, Mi et al. [24] have studied yttria-doped nickel hydroxide as the positive electrode of Ni-MH batteries and concluded that the high-temperature performance was improved due to the formation of an yttria-rich surface layer, and that the optimum amount of yttria was around 1% to obtain a high-discharge capacity at 60 °C.

In the positive electrode of Ni-MH batteries, the oxidization potential of  $\text{Ni}(\text{OH})_2$  and the oxygen evolution potential can par-

\* Corresponding author. Tel.: +1 519 253 3000x4785; fax: +1 519 973 7007.  
E-mail address: [dnorthwo@uwindsor.ca](mailto:dnorthwo@uwindsor.ca) (D.O. Northwood).

tially overlap. Therefore, when charging Ni-MH batteries, the oxygen evolution reaction will use part of the charging current. This situation becomes worse at higher temperatures because the oxygen evolution potential decreases. Ca has been shown to be an effective addition to increase the oxygen evolution potential [25] and therefore, the charge acceptance of the positive electrode can be increased with the addition of Ca, especially at high temperatures. Recently, He et al. [26] coated  $\text{Ca}_3(\text{PO}_4)_2$  on the  $\text{Ni}(\text{OH})_2$  and found that the discharge capacity of nickel hydroxide was improved because of the increase in the oxygen evolution potential.

Although Y- [24] or Ca- [26] coated  $\text{Ni}(\text{OH})_2$  can significantly improve the high-temperature characteristics, the use of such a coating technology will also increase the cost of Ni-MH batteries. Therefore, finding another relatively cheap and easy method to increase the high-temperature charge acceptance of the positive electrode is very important to the further commercialization of Ni-MH batteries. In this study, calcium fluoride was added directly to the pasted nickel hydroxide electrode. The results show that a  $\text{CaF}_2$  addition to the nickel hydroxide electrode improved both the high-temperature charge acceptance and the charge/discharge cycling stability at higher temperatures.

## 2. Experimental details

Cobalt sulfate and sodium hydroxide were used to react with the spherical nickel hydroxide powder in a reaction vessel to precipitate cobalt hydroxide on the surface of the nickel hydroxide particles. The reaction pH was maintained 9–10 by a PH meter. The reaction temperature was controlled at around 50 °C. A more detailed description of the surface modification of the nickel hydroxide powder can be found in Ref. [27]. The  $\text{Co}(\text{OH})_2$ -coated nickel hydroxide powder was continuously treated in a hot alkaline solution. The alkaline solution contains 25–45 wt.% sodium hydroxide. The temperature of alkaline treatment was 110–120 °C. The hot alkaline treatment leads to an increase in the stability of cobalt layer on the surface of the nickel hydroxide particles. The content of cobalt hydroxide at the surface of nickel hydroxide particle was 6.5 wt.%. The  $\text{Co}(\text{OH})_2$ -coated nickel hydroxide powder was then used to paste the positive electrode of the Ni-MH batteries.

The paste composition of nickel hydroxide electrode is 5–7 wt.% Co, 2–5 wt.% Zn, 0.2–1.0 wt.% Ca, 0.15 wt.% PTFE and balance  $\text{Ni}(\text{OH})_2$ . In the pasted nickel hydroxide electrode, the cobalt plays an important role in the electrode conductivity, capacity utilization and durability. The zinc is used to decrease the nickel electrode swelling and increase the cycle lifetime of the pasted nickel electrode. As previously discussed, the calcium addition was used to improve the high-temperature charge acceptance of the pasted nickel electrode. The calcium fluoride was first mixed with cobalt powder in a weight ratio of 1:1 and then the mixture of cobalt and calcium fluoride was added into the pasted nickel electrode. PTFE was used as the binding material. The metal hydride electrode was composed of hydrogen-absorbing alloy powder (MmNi<sub>5</sub>-based alloy), conductive carbon powder, binding materials and the punched metal sheet. The punched metal sheet is made from the

nickel-coated stainless steel strip or pure nickel strip (thickness: 0.045 mm). The paste composition of the metal hydride electrode is 98.85 wt.% MH powder, 0.3 wt.% carbon, 0.85 wt.% binding materials.

The dimensions of the pasted nickel electrode plate for manufacturing the Ni-MH batteries were 281 mm × 33 mm × 0.5 mm and the dimensions of the pasted MH electrode plate were 360 mm × 33 mm × 0.3 mm. The thickness of the polypropylene separator was 0.12 mm. The capacity of the negative electrode plate was designed to be 1.5 times higher than that of the positive electrode. The electrolyte in the cells was a 6 M KOH and 1 M LiOH aqueous solution. The weight of the electrolyte in each cell was 4.8 g. The charge/discharge tests of the Ni-MH cells were conducted at temperatures ranging from 20 °C to 60 °C.

The gas in the batteries was collected using a special apparatus, which was set up in a 60 °C oven. A hole was drilled at the top of battery, which was put in a volumetric tube filled with mineral oil. When the gas released from the battery, it would be collected at the top of the tube. The batteries were in the fully charged state.

## 3. Results and discussion

### 3.1. Effects of $\text{Co}(\text{OH})_2$ -coating on $\text{Ni}(\text{OH})_2$ powder

The nickel hydroxide particles used in this work have a surface layer of cobalt hydroxide. The cobalt hydroxide has a cobalt valence of 2.0. It is preferable to employ cobalt oxide having a cobalt valence over 3.0 (e.g.,  $\gamma$ -cobalt oxyhydroxide ( $\text{CoOOH}$ )) because it is not easily reduced by overdischarge. Fig. 1 shows the specific discharge capacity of the “regular” nickel hydroxide and  $\text{Co}(\text{OH})_2$ -coated nickel hydroxide particles. The specific discharge capacity of the regular nickel hydroxide powder reaches a value of 264.3  $\text{mAh g}^{-1}$  after four cycles. The specific discharge capacity of the  $\text{Co}(\text{OH})_2$ -coated  $\text{Ni}(\text{OH})_2$  powder (6.5 wt.% cobalt hydroxide on the surface of  $\text{Ni}(\text{OH})_2$

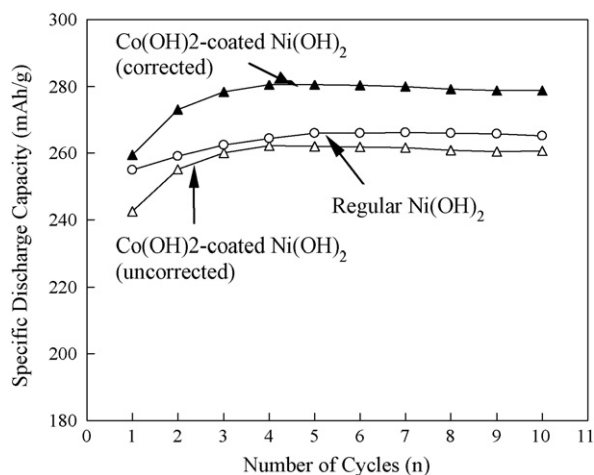


Fig. 1. Specific discharge capacity of  $\text{Co}(\text{OH})_2$ -coated  $\text{Ni}(\text{OH})_2$  and “regular”  $\text{Ni}(\text{OH})_2$  as a function of cycle lifetime (charge: 0.1 C, 15h; rest: 1h; discharge: 0.2 C to 1 V end-of-discharge voltage).

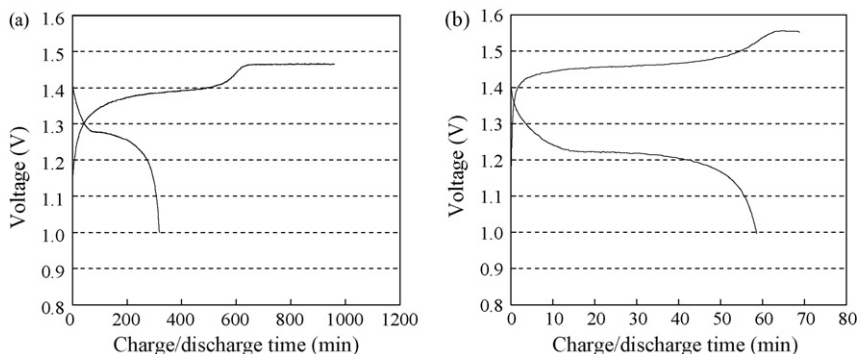


Fig. 2. Charge/discharge curves of Ni-MH batteries at room temperature: (a) charge 0.1 C  $\times$  16 h and discharge at 0.2 C to an end-of-discharge voltage of 1.0 V and (b) charge 1 C to end-of-charge of  $-\Delta V=5\text{mV}$  and discharge at 1 C to an end-of-discharge voltage of 1.0 V.

powder) reaches a value of  $262.2\text{mAh g}^{-1}$  after four cycles. The discharge capacity of  $\text{Co}(\text{OH})_2$ -coated nickel hydroxide particles was then corrected to reflect the actual  $\text{Ni}(\text{OH})_2$  content (93.5%  $\text{Ni}(\text{OH})_2$  in the  $\text{Co}(\text{OH})_2$ -coated  $\text{Ni}(\text{OH})_2$  powder). The corrected specific discharge capacity of  $\text{Ni}(\text{OH})_2$  in  $\text{Co}(\text{OH})_2$ -coated  $\text{Ni}(\text{OH})_2$  powder was  $280\text{mAh g}^{-1}$ . The capacity utilization of the  $\text{Ni}(\text{OH})_2$  in the  $\text{Co}(\text{OH})_2$ -coated nickel hydroxide powder has, therefore, been improved in comparison to the “regular” nickel hydroxide powder.

### 3.2. Charge–discharge characteristics of Ni-MH batteries made with $\text{Co}(\text{OH})_2$ -coated $\text{Ni}(\text{OH})_2$

Fig. 2 shows the charge and discharge curves of the Ni-MH batteries (nominal capacity: 2700 mAh) at room temperature. The discharge capacity of these cells is over 2700 mAh at 0.2 C discharge current. The discharge capacity of these cells at 1 C discharge current is over 2600 mAh. Fig. 3 shows the discharge capacity of the Ni-MH batteries as a function of the number of charge/discharge cycles. The charge/discharge cycling tests were conducted at 2600 mA charge current to end-of-charge voltage deficiency ( $-\Delta V=5\text{mV}$ ) and 10 A discharge current to an end-of-discharge voltage of 0.9 V. The manufacturer of

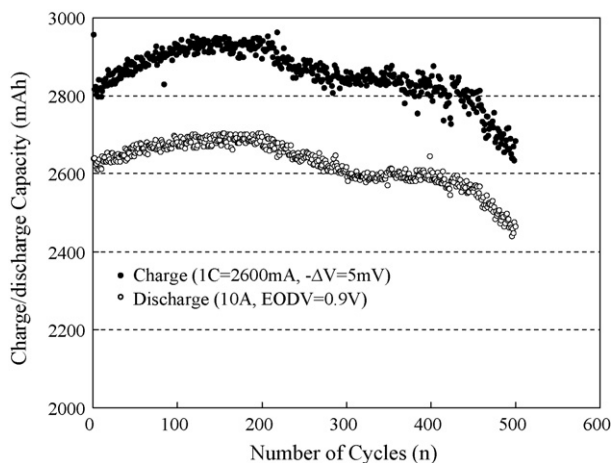


Fig. 3. Charge/discharge capacity of Ni-MH batteries as a function of the number of charge/discharge cycles (charge 1 C to end-of-charge of  $-\Delta V=5\text{mV}$  and discharge at 10 A to an end-of-discharge voltage of 0.9 V).

Ni-MH batteries aims at achieving a good high-temperature charge acceptance. An increase in oxygen evolution potential of the nickel electrode leads to an increase in the high-temperature charge acceptance. The maximum overcharge voltage reflects the oxygen evolution potential of the nickel hydroxide electrode. It has been found that the discharge capacity of the Ni-MH cell remains almost constant at a value of 2600 mAh during the first 400 cycles, but decreases to about 2450 mAh after 500 cycles.

### 3.3. Effect of $\text{CaF}_2$ addition on the charge/discharge characteristics of Ni-MH cells

Fig. 4 shows the charge/discharge curves at different temperatures of Ni-MH cells made using nickel electrodes with and without a  $\text{CaF}_2$  addition. These cells were charged at 1 C charge current at different temperatures to an end-of-charge voltage deficiency ( $-\Delta V=5\text{mV}$ ). After resting 10 min at each temperature, the charged cell was discharged at 1 C discharge current at temperature to an end-of-discharge voltage of 1.0 V. It can be clearly seen that the high-temperature charge acceptance of the Ni-MH cell made using the  $\text{CaF}_2$ -containing nickel electrode remains almost constant at temperatures ranging from  $20^\circ\text{C}$  to  $50^\circ\text{C}$ . The high-temperature charge acceptance (%) was calculated using the ratio (the discharge capacity at high temperature for a high-temperature charged cell/the discharge capacity at  $20^\circ\text{C}$  for a  $20^\circ\text{C}$  – charged-cell)  $\times 100\%$ .

The discharge capacity of the batteries was measured at different temperatures after charging at the same temperatures. The discharge capacity reflects the charge acceptance of the Ni-MH batteries at the given temperatures. Thus, the discharge performance of the calcium-containing nickel electrodes shows similar capacity utilization at temperatures ranging from  $20^\circ\text{C}$  to  $50^\circ\text{C}$ . The capacity utilization of a battery made using calcium-containing nickel hydroxide paste decreases by about 5% at  $60^\circ\text{C}$  compared to  $20^\circ\text{C}$ . As the oxygen evolution potential decreases at higher temperatures, the  $\text{Ni}(\text{OH})_2$  oxidation potential and the oxygen evolution potential overlap, and the charge efficiency of the positive electrode active material declines. However, through the addition of calcium to the nickel electrode paste, the decrease in the oxygen evolution potential at higher temperatures is retarded and thus there is an improvement in the high-temperature charge efficiency. As shown in Fig. 4(b),

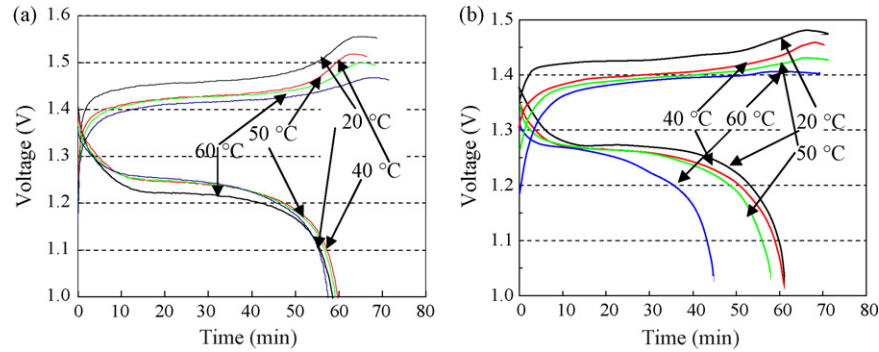


Fig. 4. Typical charge/discharge curves of Ni-MH cells at different temperatures (charge: 1 C to end-of-charge at  $-\Delta V=10$  mV; rest: 10 min; discharge: 1 C to end-of-discharge voltage 1.0 V) (nickel electrodes: (a) with  $\text{CaF}_2$  addition and (b) without  $\text{CaF}_2$  addition).

the capacity utilization of the Ni-MH batteries made using the  $\text{Co}(\text{OH})_2$ -coated nickel hydroxide electrode without a calcium addition decreases at  $60^\circ\text{C}$  to value of 72% of that at  $20^\circ\text{C}$ .

Thus, a uniform distribution of  $\text{CaF}_2$  in the pasted nickel electrode significantly increases the high-temperature charge acceptance of the Ni-MH batteries at high temperatures (e.g.,  $60^\circ\text{C}$ ). It was noted that the overcharge voltage of the Ni-MH battery containing  $\text{CaF}_2$  reached a maximum value of 1.45 V at 1 C charge current at  $60^\circ\text{C}$ . The higher overcharge voltage at high temperatures results from the higher oxygen evolution potential produced through the addition of calcium in the nickel hydroxide electrode. The shift of oxygen evolution potential into the noble potential range leads to the increase in the high-temperature charge acceptance of Ni-MH batteries. It can be seen from Fig. 4(a) that the charge acceptance of the Ni-MH battery made with calcium-containing nickel electrode is over 95% at  $60^\circ\text{C}$ .

The high-temperature charge acceptance of Ni-MH batteries is mainly dependent on the surface composition of nickel hydroxide particles and the manufacturing technology used for the production of the pasted nickel electrode. At the beginning of the charge/discharge cycling, the capacity utilization of Ni-MH battery was over 98% at  $60^\circ\text{C}$ . However, the capacity utilization of the Ni-MH batteries at  $60^\circ\text{C}$  slightly decreases to a value of about 92% after 10 cycles. This small degradation in capacity utilization of the Ni-MH cells reflects the instability of the Ni-MH battery at higher temperatures. Fig. 5(a) shows the charge/discharge curves of Ni-MH cells at  $60^\circ\text{C}$

at different charge/discharge cycles. The maximum overcharge voltage slightly decreases with increasing number of cycles. The decrease in overcharge voltage on cycling leads to an increase in the oxygen evolution potential and a stabilization of the Ni-MH battery characteristics. The very small variations in the maximum overcharge voltage with increasing number of cycles at  $60^\circ\text{C}$  reflect the stability and durability of the Ni-MH cells. There was a decrease in overcharge voltage of about 4 mV after the first cycle at  $60^\circ\text{C}$ . Then, the maximum overcharge voltage remains almost constant (change is less than 0.5 mV) up to 10 cycles. This decrease in the overcharge voltage at  $60^\circ\text{C}$  results from a decrease in the overcharge oxygen evolution potential. The discharge capacity instability of the Ni-MH batteries at higher temperatures is related to the fast oxygen evolution during the overcharge process and to the battery temperature quickly rising over  $60^\circ\text{C}$ . Also, the discharge capacity is gradually reduced with increasing the cycle number because the discharge capacity of Ni-MH battery is very hard to stabilize at  $60^\circ\text{C}$ , especially at overcharge condition at high temperature.

This cycling instability of Ni-MH batteries at high temperatures reflects the instability of the electrochemical characteristics of the pasted nickel electrode. The stability of conductive  $\text{CoOOH}$  layer on the surface of nickel hydroxide powder at higher temperatures predominantly determines the durability of Ni-MH batteries. For nickel hydroxide active material having high-order cobalt compound layers on the surface, the conductive  $\text{CoOOH}$  network at the surface of nickel hydroxide powder becomes unstable at higher temperatures. As a result,

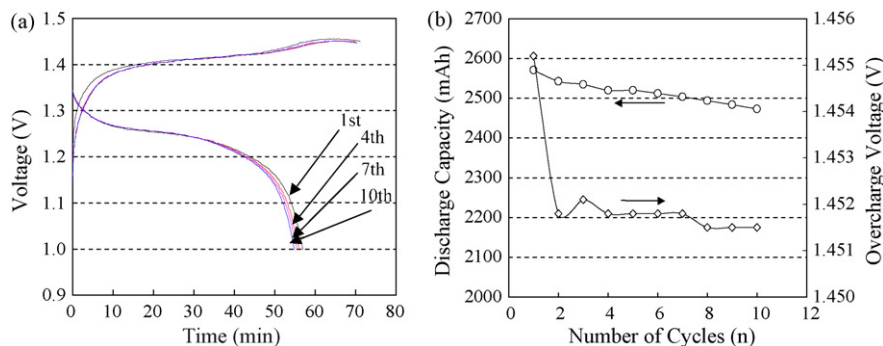


Fig. 5. (a) Charge/discharge curves of Ni-MH cells as a function of number of cycles at  $60^\circ\text{C}$  (charge: 1 C to an end-of-charge voltage deficiency  $-\Delta V=5$  mV; rest 15 min; discharge: 1 C to EODV 1.0 V; rest 10 min; recharge). (b) Maximum overcharge voltage and discharge capacity vs. number of cycles plots.



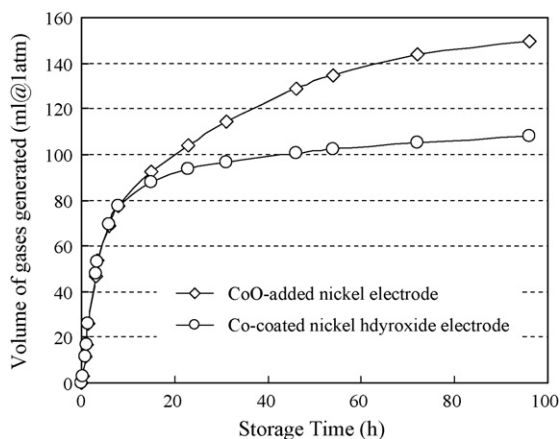


Fig. 6. Gassing evolution volumes of the charged Ni-MH cells using Co-coated nickel hydroxide electrode and CoO-added nickel electrode at 60 °C storage. Both electrodes contain 0.5 wt.% CaF<sub>2</sub>.

the amount of cobalt on the surfaces decreases, thus reducing the conductive network within the nickel electrode, thereby decreasing the capacity of the cell. The anti-corrosive capability of the hydrogen-absorbing alloy particles in the negative electrode decreases at higher temperatures. Metallic elements such as Mn and Al in the metal hydride alloy powders are dissolved and move to the positive electrode side where they degrade the conductive CoOOH networks at the surface of nickel hydroxide powders. The dissolved metallic elements readily form small crystallites on the inside separator and these small crystallites lead to short-circuiting of the battery at high temperatures. Thus, any improvement of stability and durability of Ni-MH batteries at higher temperatures is focused on increasing the charge acceptance of the nickel electrode and decreasing the elemental dissolution at the surface of the metal hydride particles.

### 3.4. Gas release in Ni-MH cells containing CaF<sub>2</sub>

The stability of the nickel electrode at higher temperature plays an important role in determining a battery's high-rate charge/discharge capability. This instability can be reflected in terms of gas release and build-up of inner pressure in the battery. In this study, charged Sc (IEC HR 23/43) Ni-MH cells were opened up and we have collected the gassing volume of the battery at 60 °C. We had controlled the weight and dimensions of the positive and negative electrodes in the two different cells examined. Two different positive electrodes were used, Co(OH)<sub>2</sub>-coated nickel hydroxide electrode and CoO additives to the nickel hydroxide. Both nickel electrodes contained 0.5 wt.% CaF<sub>2</sub>. It was shown that the battery gassing at beginning of storage mainly comes from the hydrogen evolution in the negative MH electrode. After storing for about 10 h, the battery gassing mainly results from the decomposition of nickel and cobalt compound materials in the positive electrode and the instability results in oxygen evolution. From Fig. 6 it can be seen that the rate of increase in volume of gases in the Ni-MH cell made using Co(OH)<sub>2</sub>-coated nickel hydroxide electrode remains at about 0.15 ml h<sup>-1</sup> after 2-day storage at 60 °C. However, the rate of increase in volume of gases in the Ni-MH cell with the

CoO-added nickel hydroxide electrode is about 0.42 ml h<sup>-1</sup> after 2-day storage at 60 °C. Thus, the use of a Co(OH)<sub>2</sub>-coated nickel hydroxide electrode is also beneficial for the positive electrode stability during high-temperature storage.

## 4. Conclusions

The addition of CaF<sub>2</sub> to the nickel electrode of a Ni-MH battery led to superior high-temperature charge/discharge performance. The charge acceptance of the CaF<sub>2</sub>-containing battery reached over 90% at 60 °C after 10 charge/discharge cycles. The use of Co(OH)<sub>2</sub>-coated Ni(OH)<sub>2</sub> with a CaF<sub>2</sub> addition led to lower rates of gas(O<sub>2</sub>) release compared to that for CoO-added Ni(OH)<sub>2</sub> positive electrodes. These improvements in high-temperature performance of Ni-MH batteries obtained through the addition of CaF<sub>2</sub> to the positive electrode will make Ni-MH batteries more attractive for power-use applications.

## References

- [1] A. Taniguchi, N. Fujioka, M. Ikoma, A. Ohta, J. Power Sources 100 (2001) 117–124.
- [2] M.W. Verbrugge, R.S. Conell, J. Electrochem. Soc. 149 (2002) A45–A53.
- [3] U. Köhler, J. Kumpers, M. Ullrich, J. Power Sources 105 (2002) 139–144.
- [4] Q. Song, C. Chiu, S. Chan, Electrochim. Acta 51 (2006) 6548–6555.
- [5] S.R. Ovshinsky, M.A. Fetcenko, Appl. Phys. A 72 (2001) 239–244.
- [6] U. Köhler, J. Kumpers, M. Ullrich, J. Power Sources 105 (2002) 139–144.
- [7] M.L. Soria, J. Chacon, J.C. Hernandez, D. Moreno, A. Ojeda, J. Power Sources 96 (2001) 68–75.
- [8] T. Ying, X. Gao, W. Hu, F. Wu, D. Noréus, Int. J. Hydrogen Energy 31 (2006) 525–530.
- [9] R.D. Armstrong, G.W.D. Griggs, E.A. Charles, J. Appl. Electrochem. 18 (1988) 215–219.
- [10] A. Yuan, S. Cheng, J. Zhang, C. Cao, J. Power Sources 77 (1999) 178–182.
- [11] W. Zhu, J. Ke, H. Yu, D. Zhang, J. Power Sources 56 (1995) 75–79.
- [12] K. Watanabe, N. Kumagai, J. Power Sources 76 (1998) 167–174.
- [13] S. Cheng, A. Yuan, H. Liu, J. Zhang, C. Cao, J. Power Sources 76 (1998) 215–217.
- [14] K. Provazi, M.J. Giz, L.H. Dall'Antonia, S.I. Córdoba de Torresi, J. Power Sources 102 (2001) 224–232.
- [15] D.M. Constantin, E.M. Rus, L. Oniciu, L. Ghergari, J. Power Sources 74 (1998) 188–197.
- [16] J. Li, R. Li, J. Wu, H. Su, J. Power Sources 79 (1999) 86–90.
- [17] S.I. Córdoba De Torresi, Electrochim. Acta 40 (1995) 1101–1107.
- [18] A.K. Sood, J. Appl. Electrochem. 16 (1986) 274–280.
- [19] K. Watanabe, M. Koseki, N. Kumagai, J. Power Sources 58 (1996) 23–28.
- [20] V. Pralong, A. Delahaye-Vidal, B. Beaudoin, J.B. Leriche, J.M. Tarascon, J. Electrochem. Soc. 147 (2000) 1306–1313.
- [21] C. Tessier, C. Faure, L.G. Demourgues, C. Denage, G. Nabias, C. Delmas, J. Electrochem. Soc. 149 (2002) A1136–A1145.
- [22] Y. Morioka, S. Narukawa, T. Itou, J. Power Sources 100 (2001) 107–116.
- [23] M. Oshitani, M. Watada, K. Shodai, M. Kodama, J. Electrochem. Soc. 148 (2001) A67–A73.
- [24] X. Mi, X. Gao, C. Jiang, M. Geng, J. Yan, C. Wan, Electrochim. Acta 49 (2004) 3361–3366.
- [25] A. Yuan, S. Cheng, J. Zhang, C. Cao, J. Power Sources 76 (1998) 36–40.
- [26] X. He, J. Ren, W. Li, C. Jiang, C. Wan, Electrochim. Acta 51 (2006) 4533–4536.
- [27] Z. Tang, Y. Wang, M. Geng, Z. Xu, Q. Rong, Chin. J. Power Sources 28 (2004) 273–275.